Electronic Supplementary Material (ESI) for Nanoscale.


# Supporting Information

## Structural Tailoring of Nanoporous Anodic Alumina Optical Microcavities for Enhanced Resonant Recirculation of Light

**Cheryl Suwen Law[a,b,c], Siew Yee Lim[a,b,c], Andrew D. Abell[*b,c,d], Lluís F. Marsal[*e], and Abel Santos[*a,b,c]**

[a]School of Chemical Engineering, The University of Adelaide, Adelaide, SA 5005, Australia
[b]Institute for Photonics and Advanced Sensing (IPAS), The University of Adelaide, 5005 Adelaide, Australia
[c]ARC Centre of Excellence for Nanoscale BioPhotonics (CNBP), The University of Adelaide, 5005 Adelaide, Australia
[d]Department of Chemistry, The University of Adelaide, Engineering North Building, 5005 Adelaide, Australia.
[e]Department of Electronic, Electric, and Automatics Engineering, Universitat Rovira i Virgili, 43007 Tarragona, Spain

***E-Mails:** andrew.abell@adelaide.edu.au ; lluis.marsal@urv.cat ; abel.santos@adelaide.edu.au

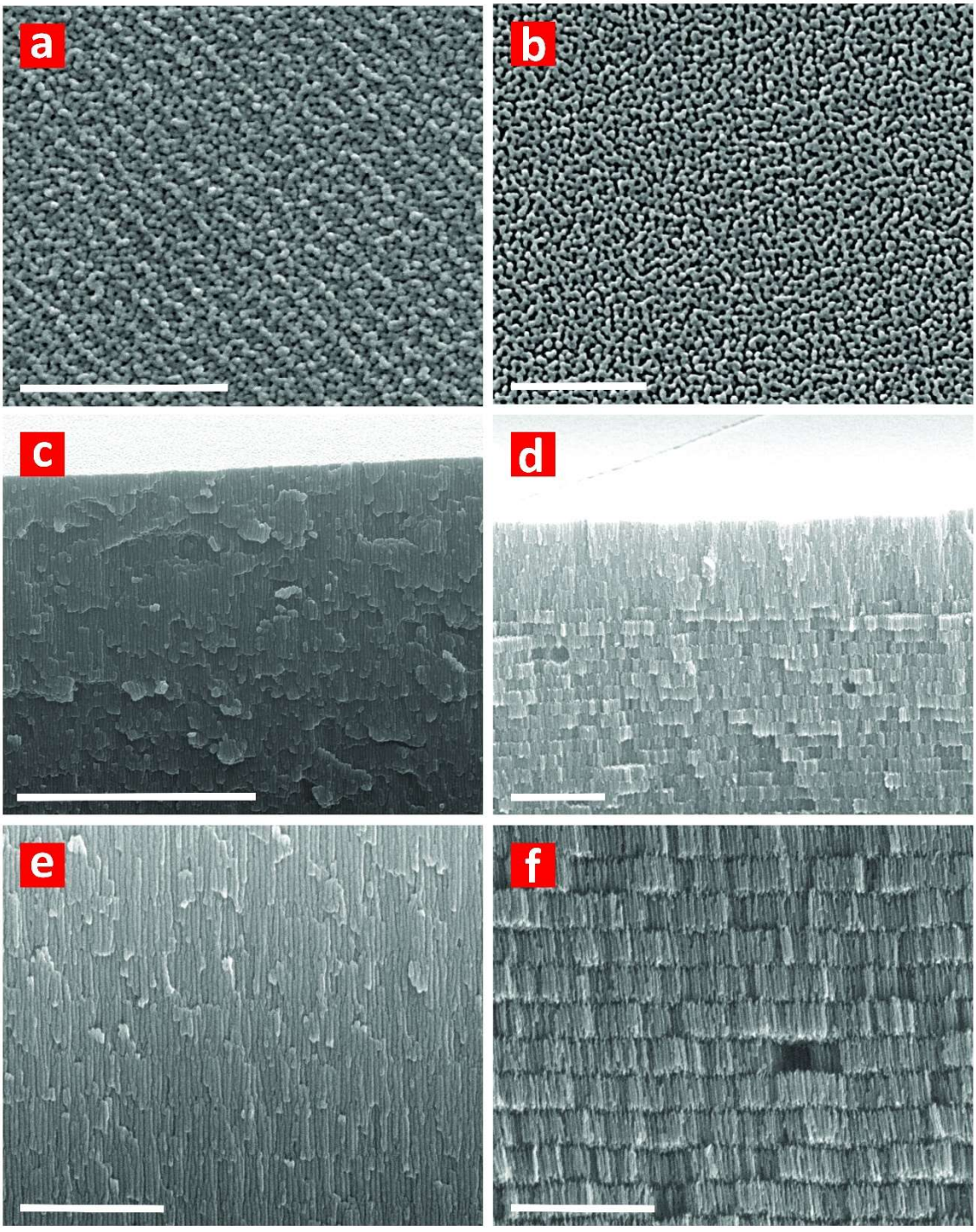


**Figure S1.** Effect of pore widening time on the structure of NAA-μCVs. a and b) Representative top view FEG-SEM images of a GIF-NAA-μCV at $t_{pw}$ = 0 and 6 min, respectively (scale bars = 500 nm). c and d) General cross-sectional view FEG-SEM images of a GIF-NAA-μCV at $t_{pw}$ = 0 and 6 min (scale bars = 2 μm). e and f) Magnified cross-sectional view FEG-SEM images showing details of the porosity contrast between layers in a GIF-NAA-μCV at $t_{pw}$ = 0 and 6 min, respectively (scale bars = 5 μm).

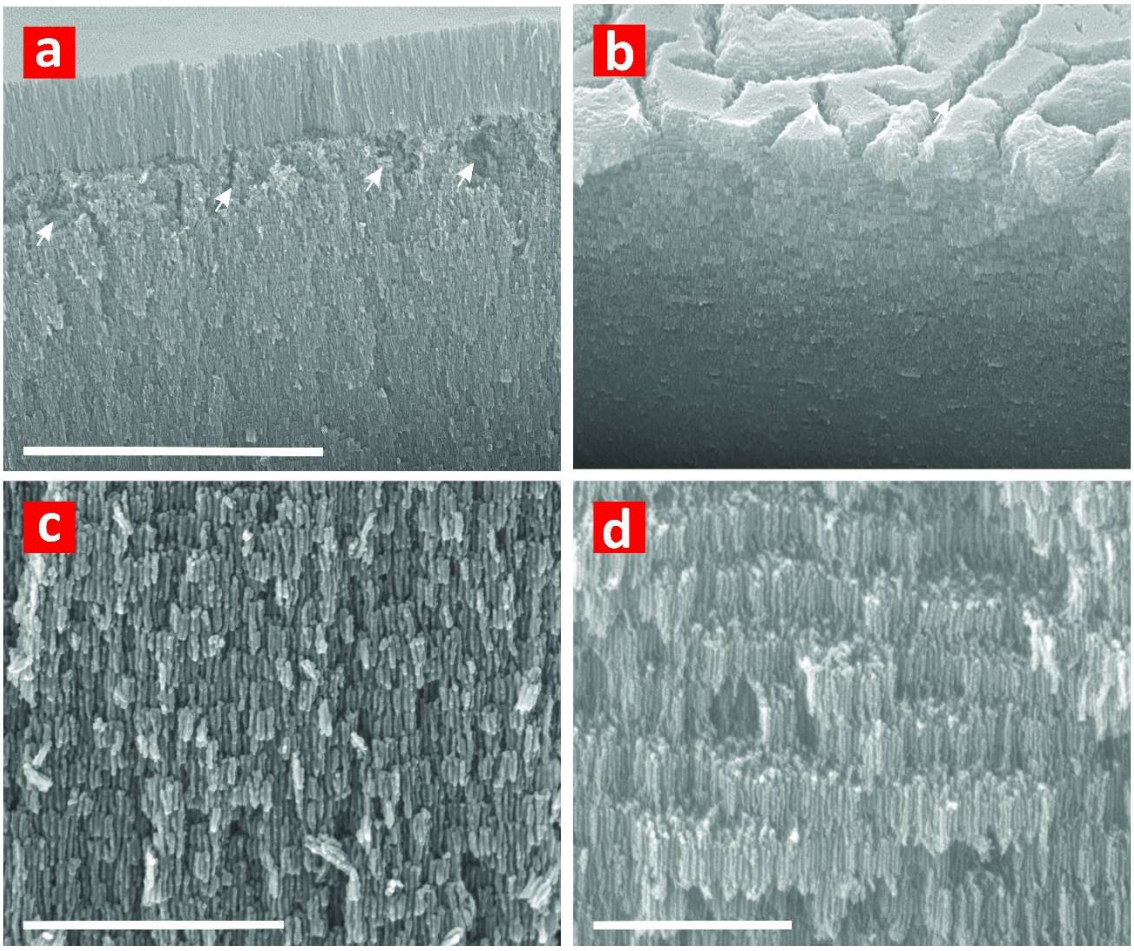


**Figure S2.** Effect of excessive pore widening time on the structure of NAA-μCVs. a and b) Representative general cross-sectional view FEG-SEM images of a GIF-NAA-μCV at $t_{pw}$ = 6 and 8 min, respectively (scale bars = 5 μm) (note: white arrows indicate regions that partially collapse due to excessive pore widening treatment). c and d) Magnified cross-sectional view FEG-SEM images showing details of the porosity between layers in a GIF-NAA-μCV at $t_{pw}$ = 6 and 8 min, respectively (scale bars = 1 μm).

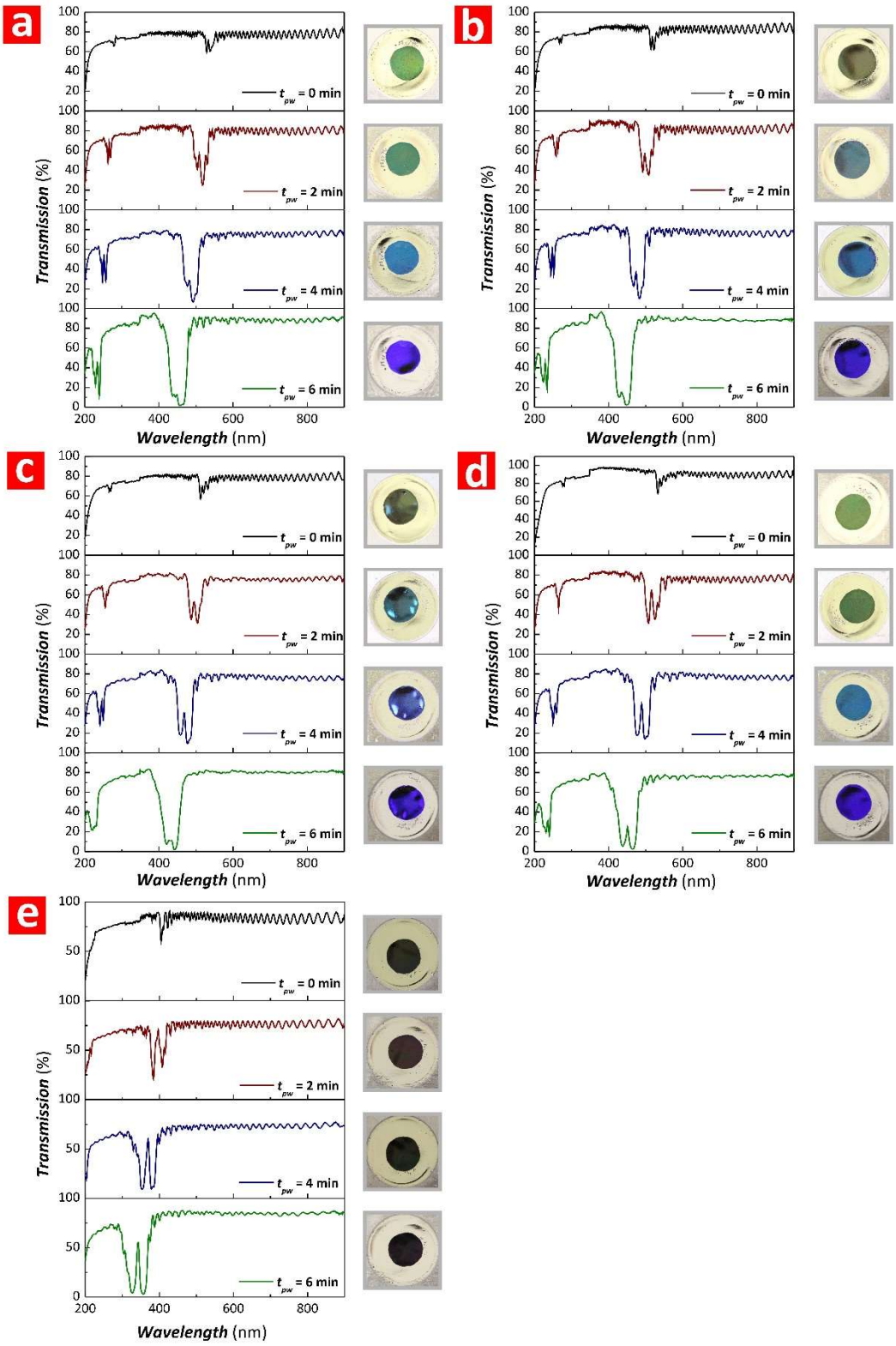


**Figure S3.** Representative transmission spectra for GIF-NAA-μCVs produced by SPA at $t_C$ = 4.5 min and variable $J_C$ and $t_{pw}$ (note: $T_P$ = 600 s, $A_J$ = 0.420 mA cm$^{-2}$, $J_{Offset}$ = 0.280 mA cm$^{-2}$, and $N_P$ = 30 pulses). a) $J_C$ = 0.210 mA cm$^{-2}$. b) $J_C$ = 0.420 mA cm$^{-2}$. c) $J_C$ = 0.315 mA cm$^{-2}$. d) $J_C$ = 0.525 mA cm$^{-2}$. e) $J_C$ = 0.630 mA cm$^{-2}$.

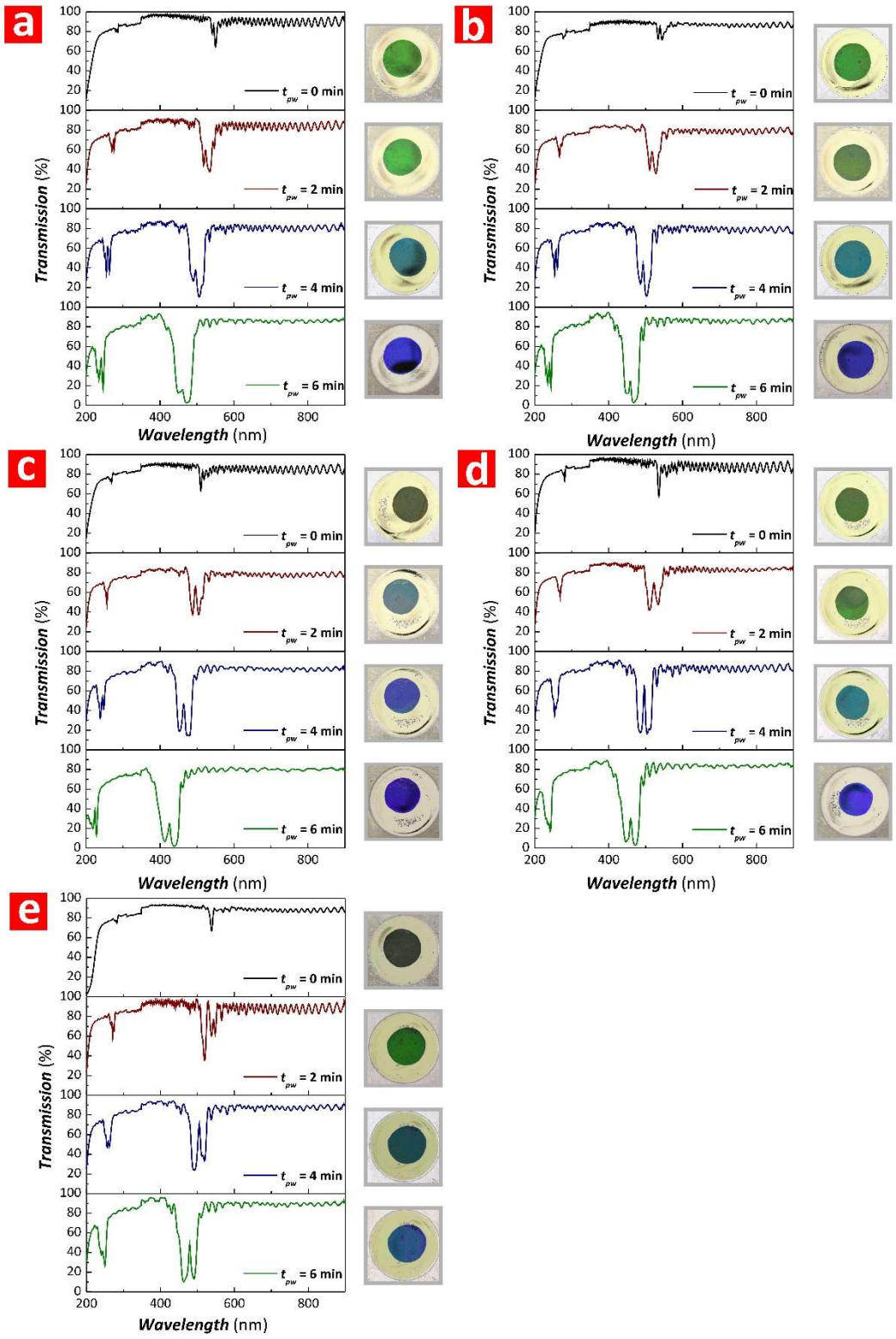


**Figure S4.** Representative transmission spectra for GIF-NAA-μCVs produced by SPA at $t_C$ = 5.5 min and variable $J_C$ and $t_{pw}$ (note: $T_P$ = 600 s, $A_J$ = 0.420 mA cm$^{-2}$, $J_{Offset}$ = 0.280 mA cm$^{-2}$, and $N_P$ = 30 pulses). a) $J_C$ = 0.210 mA cm$^{-2}$. b) $J_C$ = 0.420 mA cm$^{-2}$. c) $J_C$ = 0.315 mA cm$^{-2}$. d) $J_C$ = 0.525 mA cm$^{-2}$. e) $J_C$ = 0.630 mA cm$^{-2}$.

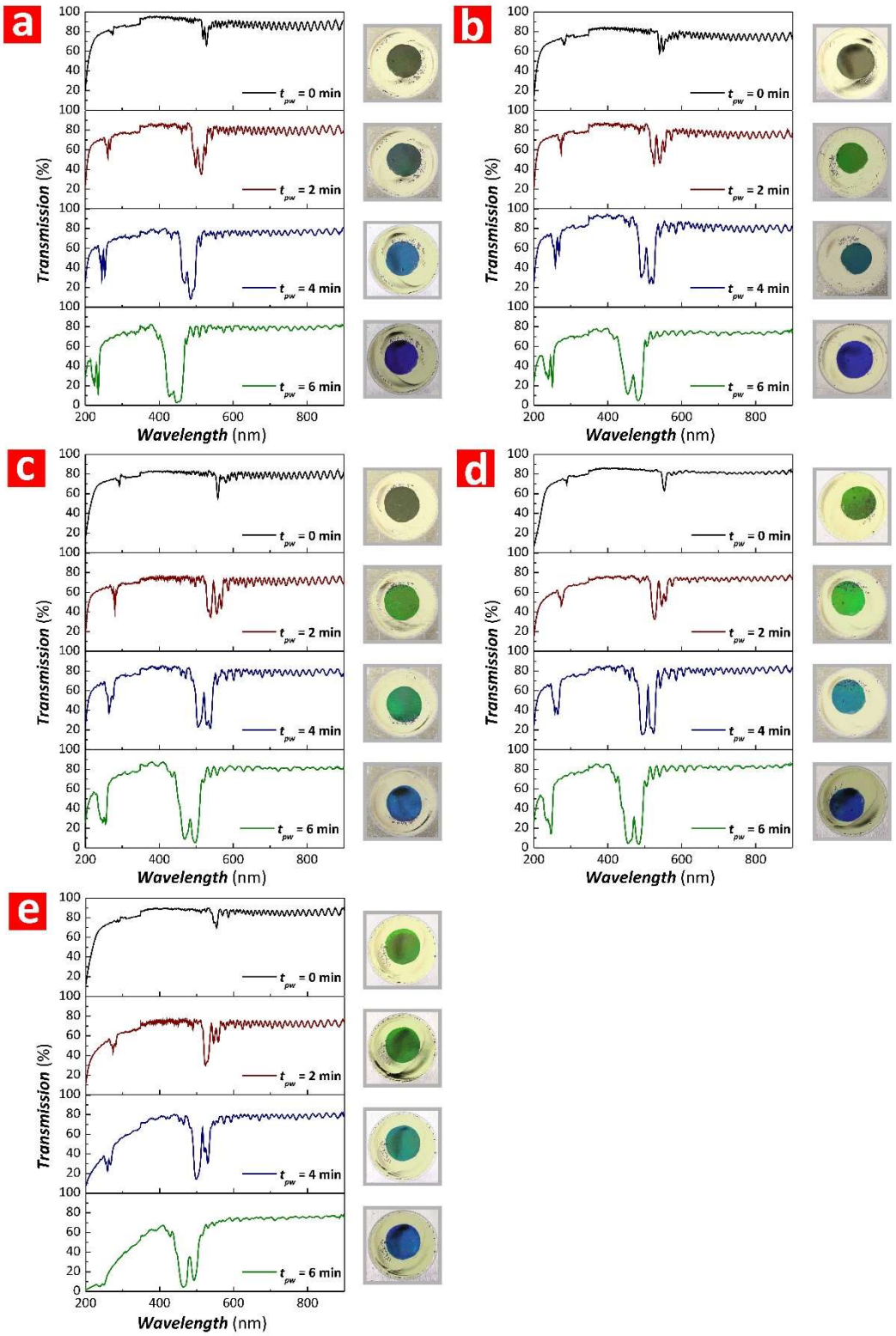


**Figure S5.** Representative transmission spectra for GIF-NAA-μCVs produced by SPA at $t_C$ = 6.5 min and variable $J_C$ and $t_{pw}$ (note: $T_P$ = 600 s, $A_J$ = 0.420 mA cm$^{-2}$, $J_{Offset}$ = 0.280 mA cm$^{-2}$, and $N_P$ = 30 pulses). a) $J_C$ = 0.210 mA cm$^{-2}$. b) $J_C$ = 0.420 mA cm$^{-2}$. c) $J_C$ = 0.315 mA cm$^{-2}$. d) $J_C$ = 0.525 mA cm$^{-2}$. e) $J_C$ = 0.630 mA cm$^{-2}$.

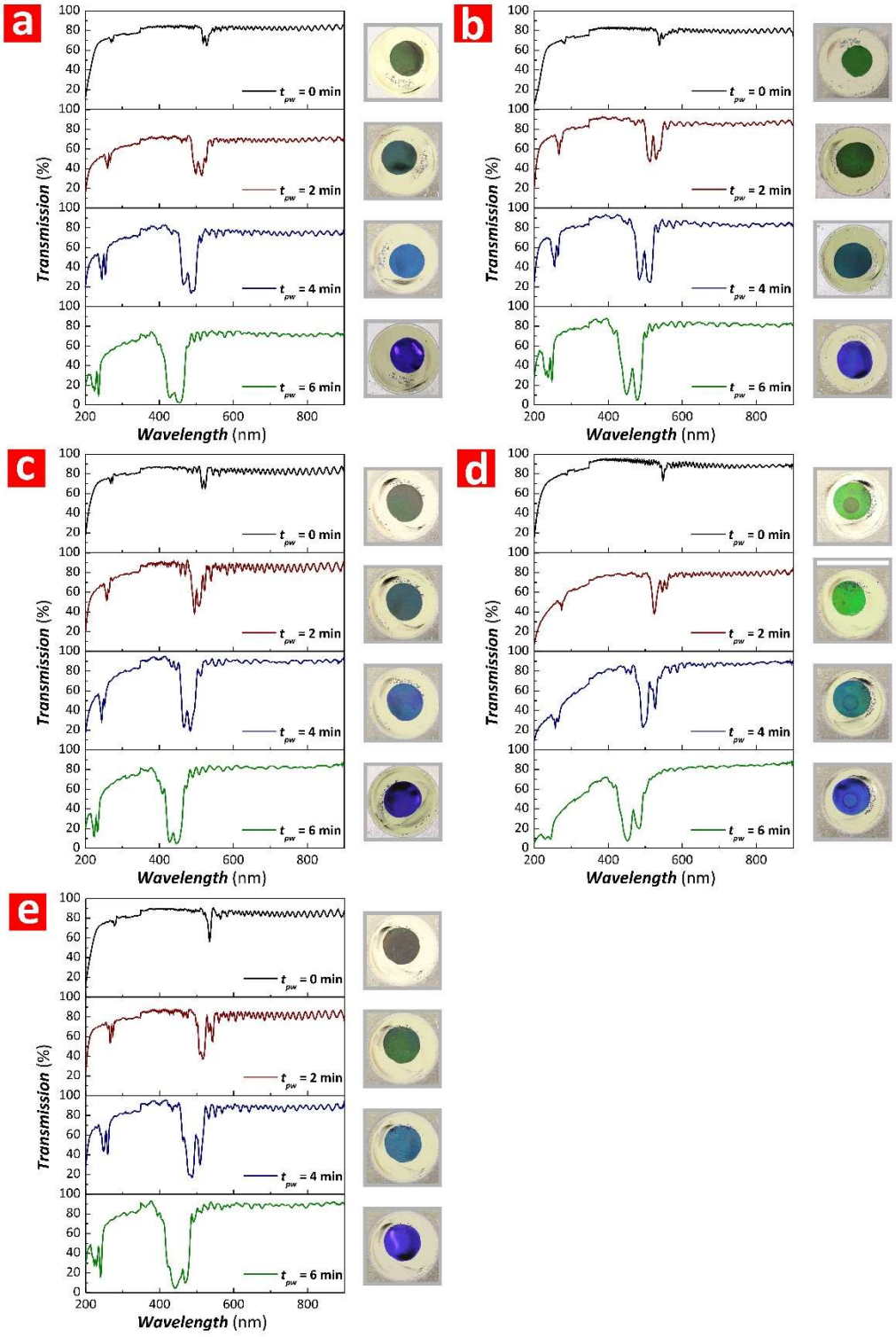


**Figure S6.** Representative transmission spectra for GIF-NAA-μCVs produced by SPA at $t_C$ = 7.5 min and variable $J_C$ and $t_{pw}$ (note: $T_P$ = 600 s, $A_J$ = 0.420 mA cm$^{-2}$, $J_{Offset}$ = 0.280 mA cm$^{-2}$, and $N_P$ = 30 pulses). a) $J_C$ = 0.210 mA cm$^{-2}$. b) $J_C$ = 0.420 mA cm$^{-2}$. c) $J_C$ = 0.315 mA cm$^{-2}$. d) $J_C$ = 0.525 mA cm$^{-2}$. e) $J_C$ = 0.630 mA cm$^{-2}$.

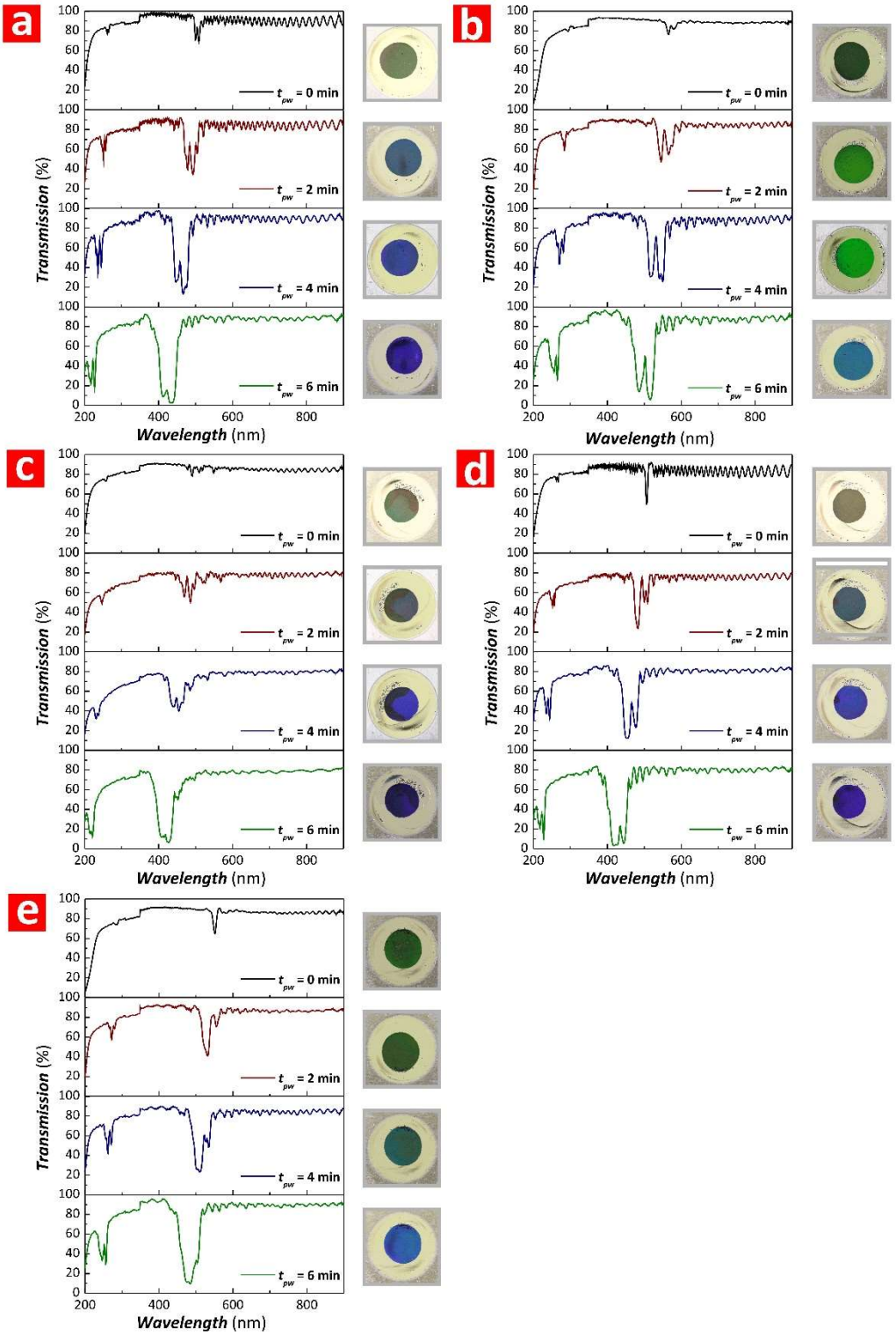


**Figure S7.** Representative transmission spectra for GIF-NAA-μCVs produced by SPA at $t_C$ = 8.5 min and variable $J_C$ and $t_{pw}$ (note: $T_P$ = 600 s, $A_J$ = 0.420 mA cm$^{-2}$, $J_{Offset}$ = 0.280 mA cm$^{-2}$, and $N_P$ = 30 pulses). a) $J_C$ = 0.210 mA cm$^{-2}$. b) $J_C$ = 0.420 mA cm$^{-2}$. c) $J_C$ = 0.315 mA cm$^{-2}$. d) $J_C$ = 0.525 mA cm$^{-2}$. e) $J_C$ = 0.630 mA cm$^{-2}$.

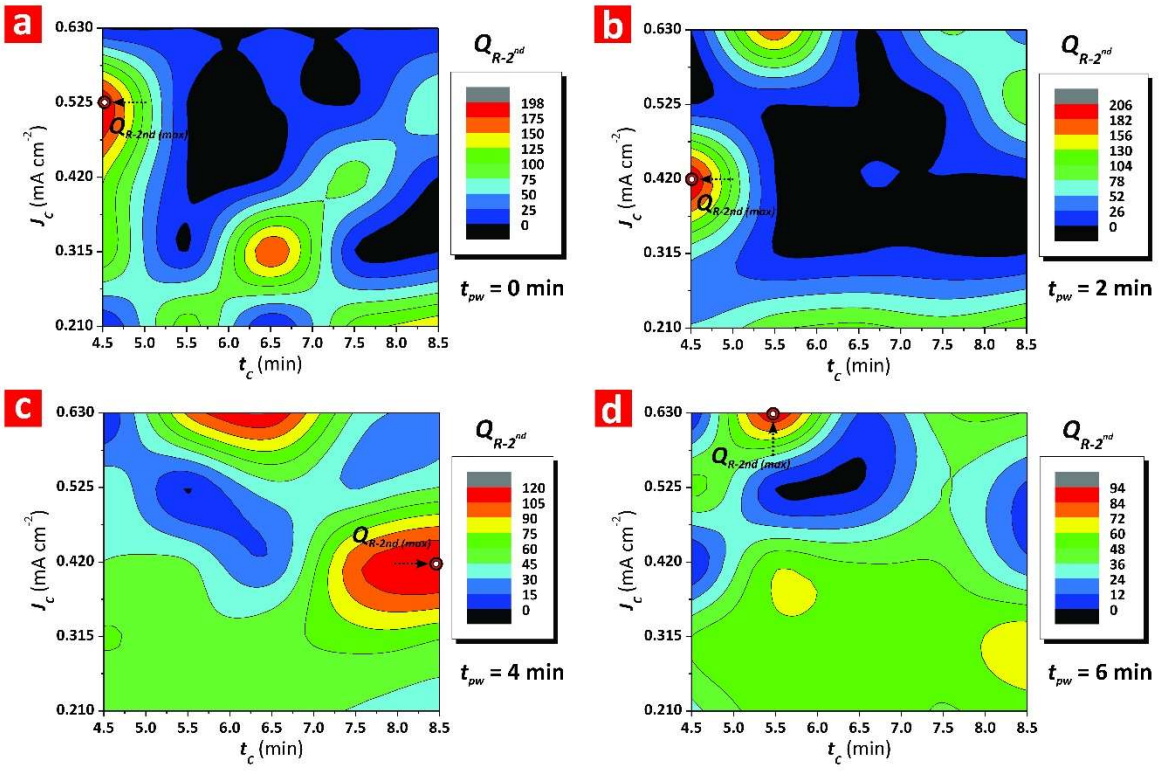


**Figure S8.** Contour maps showing the combined effect of cavity fabrication parameters (i.e. anodisation time – $t_C$ and current density – $J_C$) on the quality factor of the secon order resonance band ($Q_{R\text{-}2nd}$) of GIF-NAA-μCVs produced by SPA at different pore widening times ($t_{pw}$). a) $t_{pw}$ = 0 min. b) $t_{pw}$ = 2 min. c) $t_{pw}$ = 4 min. c) $t_{pw}$ = 6 min. (note: GIF-NAA-μCVs produced with $T_P$ = 600 s, $A_J$ = 0.420 mA cm$^{-2}$, $J_{Offset}$ = 0.280 mA cm$^{-2}$, and $N_P$ = 30 pulses).

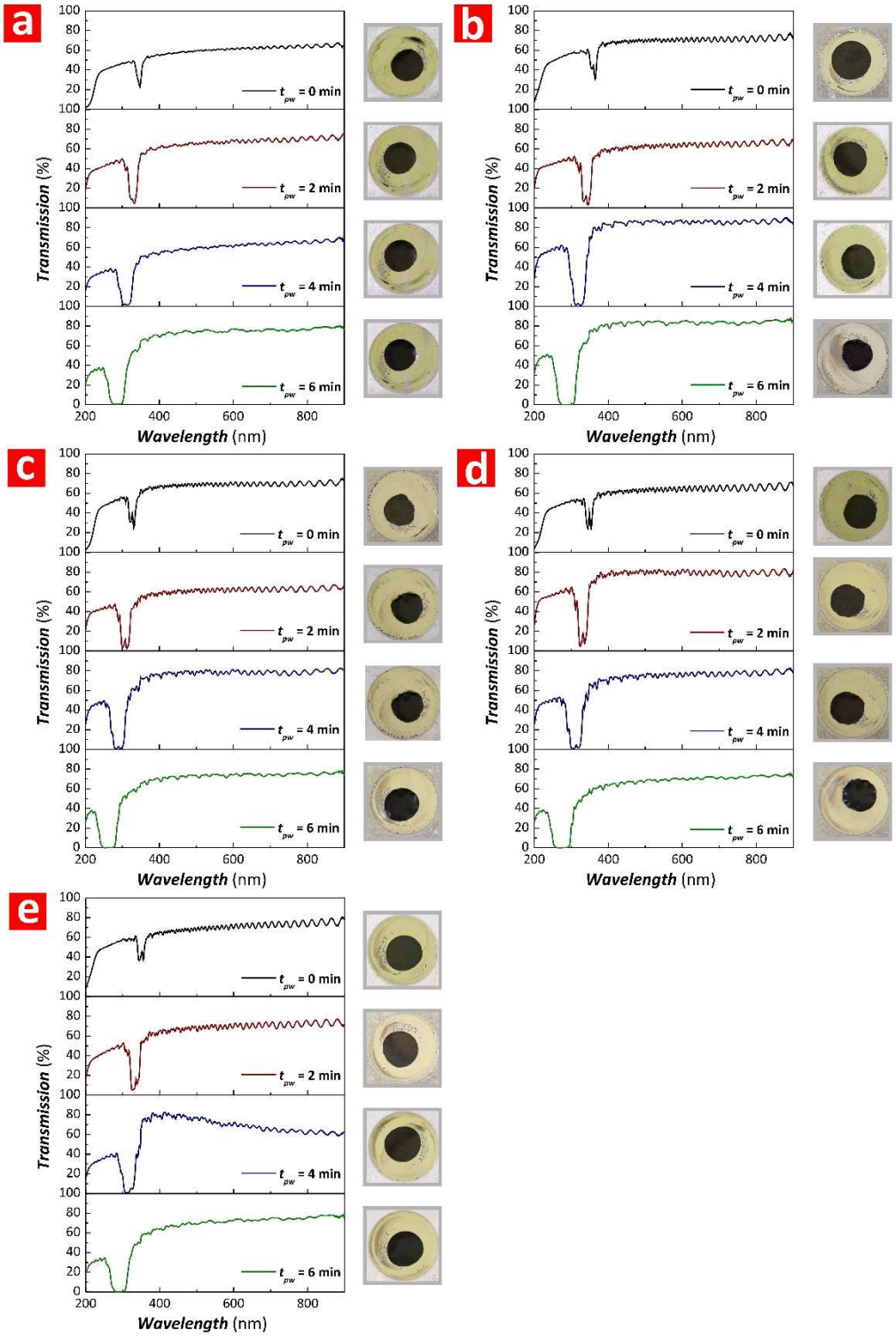


**Figure S9.** Representative transmission spectra for DBR-NAA-μCVs produced by STPA at $t_C$ = 4.5 min and variable $J_C$ and $t_{pw}$ (note: $T_P$ = 600 s, $A_J$ = 0.420 mA cm$^{-2}$, $J_{Offset}$ = 0.280 mA cm$^{-2}$, and $N_P$ = 30 pulses). a) $J_C$ = 0.210 mA cm$^{-2}$. b) $J_C$ = 0.420 mA cm$^{-2}$. c) $J_C$ = 0.315 mA cm$^{-2}$. d) $J_C$ = 0.525 mA cm$^{-2}$. e) $J_C$ = 0.630 mA cm$^{-2}$.

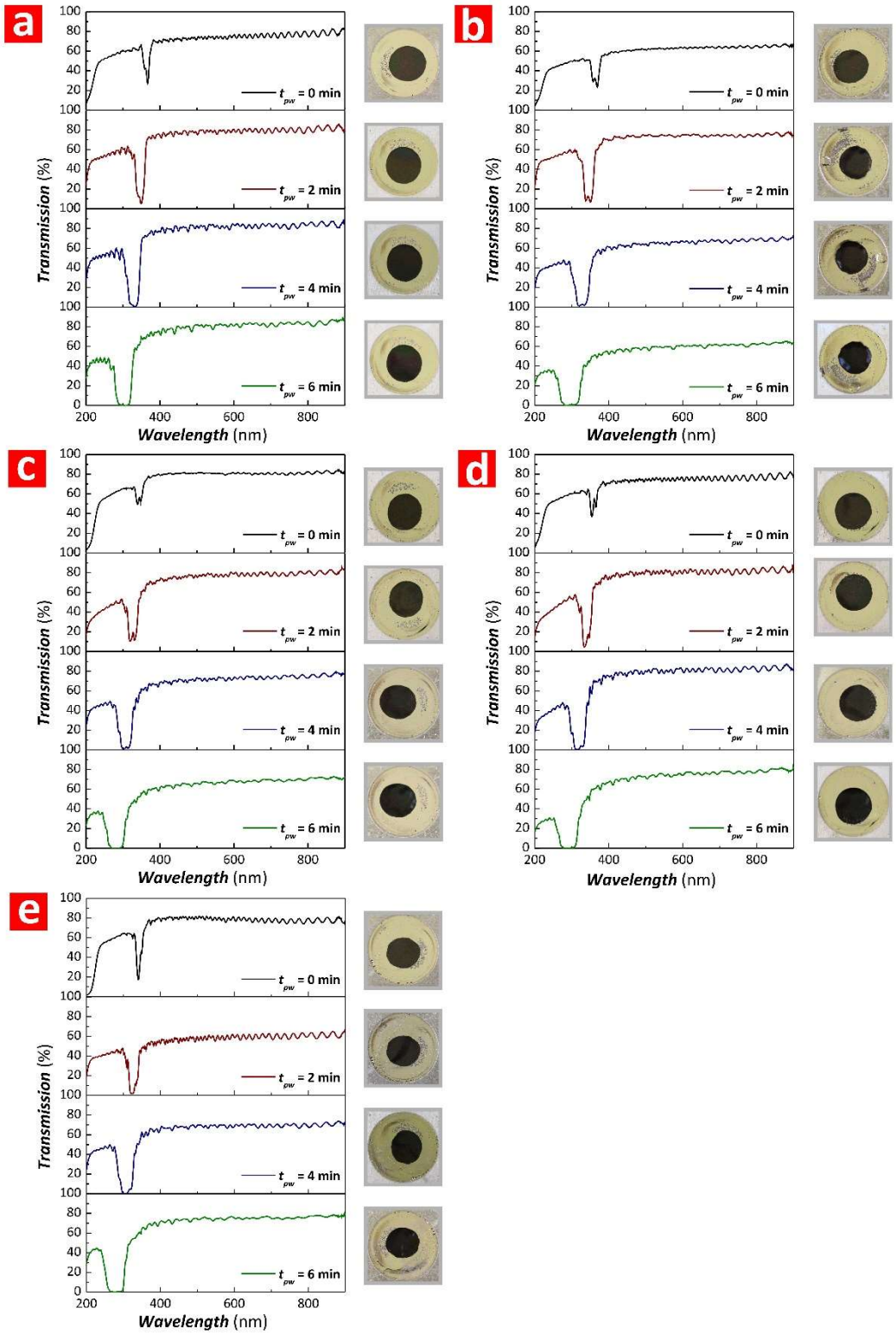


**Figure S10.** Representative transmission spectra for DBR-NAA-μCVs produced by STPA at $t_C$ = 5.5 min and variable $J_C$ and $t_{pw}$ (note: $T_P$ = 600 s, $A_J$ = 0.420 mA cm$^{-2}$, $J_{Offset}$ = 0.280 mA cm$^{-2}$, and $N_P$ = 30 pulses). a) $J_C$ = 0.210 mA cm$^{-2}$. b) $J_C$ = 0.420 mA cm$^{-2}$. c) $J_C$ = 0.315 mA cm$^{-2}$. d) $J_C$ = 0.525 mA cm$^{-2}$. e) $J_C$ = 0.630 mA cm$^{-2}$.

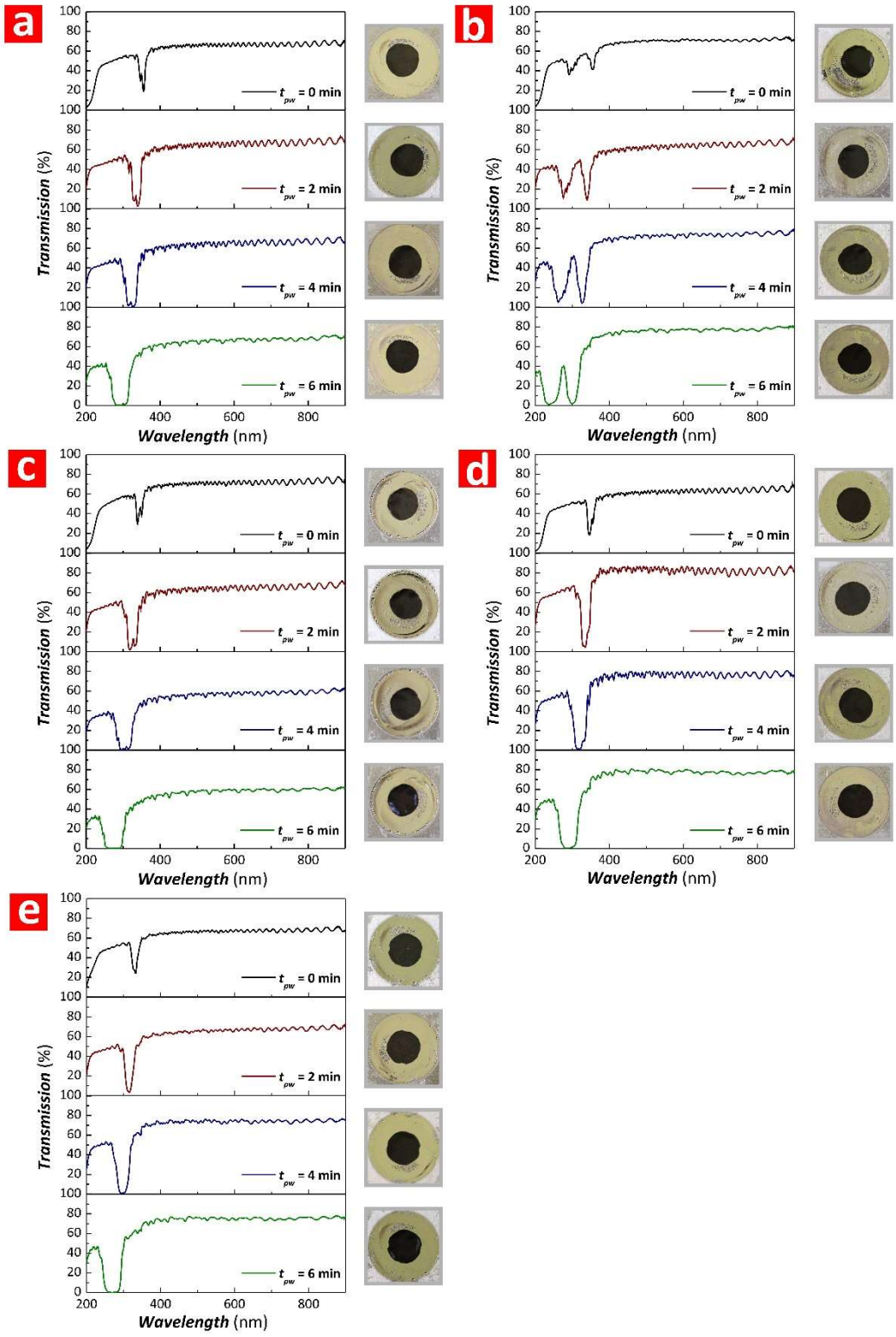


**Figure S11.** Representative transmission spectra for DBR-NAA-μCVs produced by STPA at $t_C$ = 6.5 min and variable $J_C$ and $t_{pw}$ (note: $T_P$ = 600 s, $A_J$ = 0.420 mA cm$^{-2}$, $J_{Offset}$ = 0.280 mA cm$^{-2}$, and $N_P$ = 30 pulses). a) $J_C$ = 0.210 mA cm$^{-2}$. b) $J_C$ = 0.420 mA cm$^{-2}$. c) $J_C$ = 0.315 mA cm$^{-2}$. d) $J_C$ = 0.525 mA cm$^{-2}$. e) $J_C$ = 0.630 mA cm$^{-2}$.

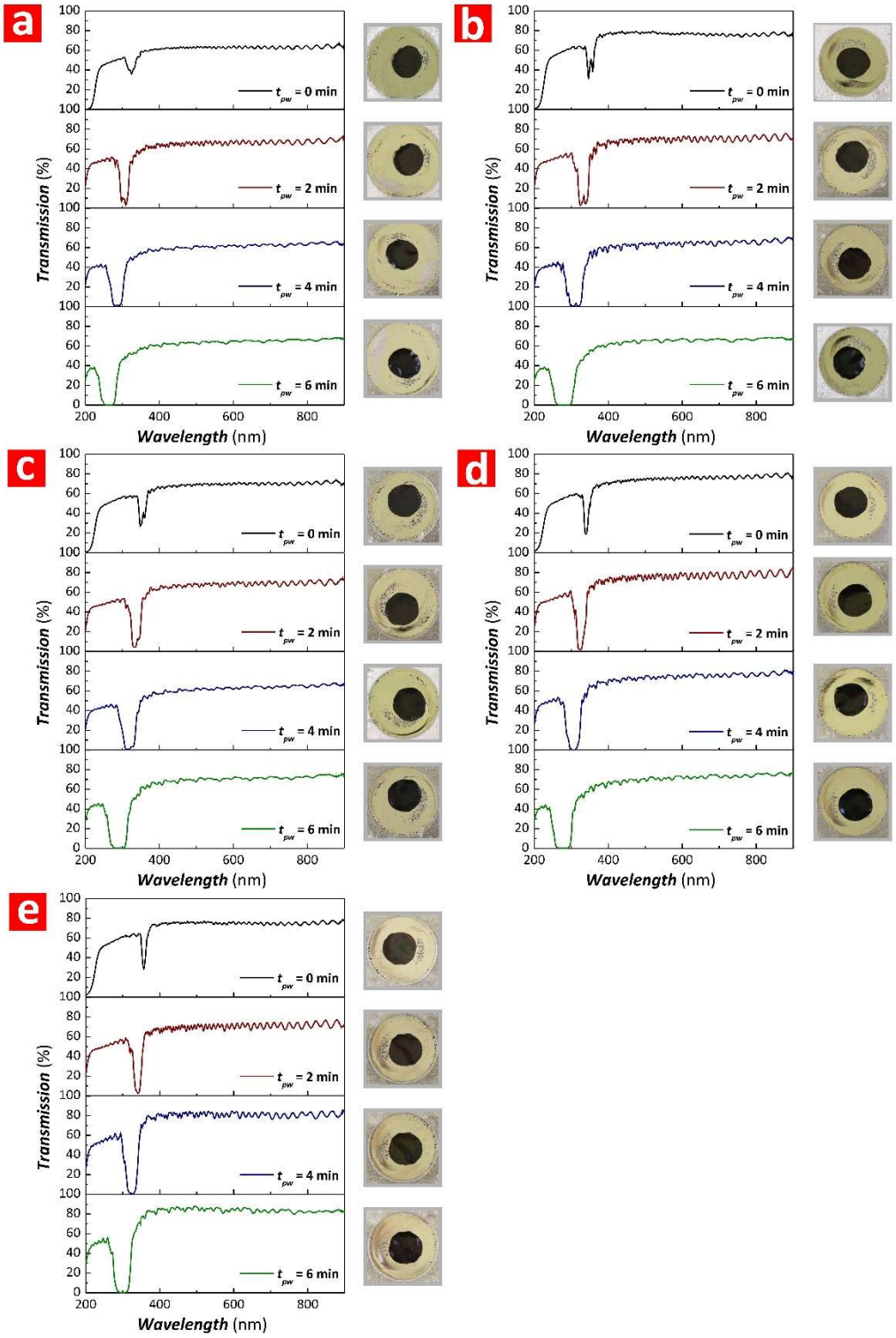


**Figure S12.** Representative transmission spectra for DBR-NAA-μCVs produced by STPA at $t_C$ = 7.5 min and variable $J_C$ and $t_{pw}$ (note: $T_P$ = 600 s, $A_J$ = 0.420 mA cm$^{-2}$, $J_{Offset}$ = 0.280 mA cm$^{-2}$, and $N_P$ = 30 pulses). a) $J_C$ = 0.210 mA cm$^{-2}$. b) $J_C$ = 0.420 mA cm$^{-2}$. c) $J_C$ = 0.315 mA cm$^{-2}$. d) $J_C$ = 0.525 mA cm$^{-2}$. e) $J_C$ = 0.630 mA cm$^{-2}$.

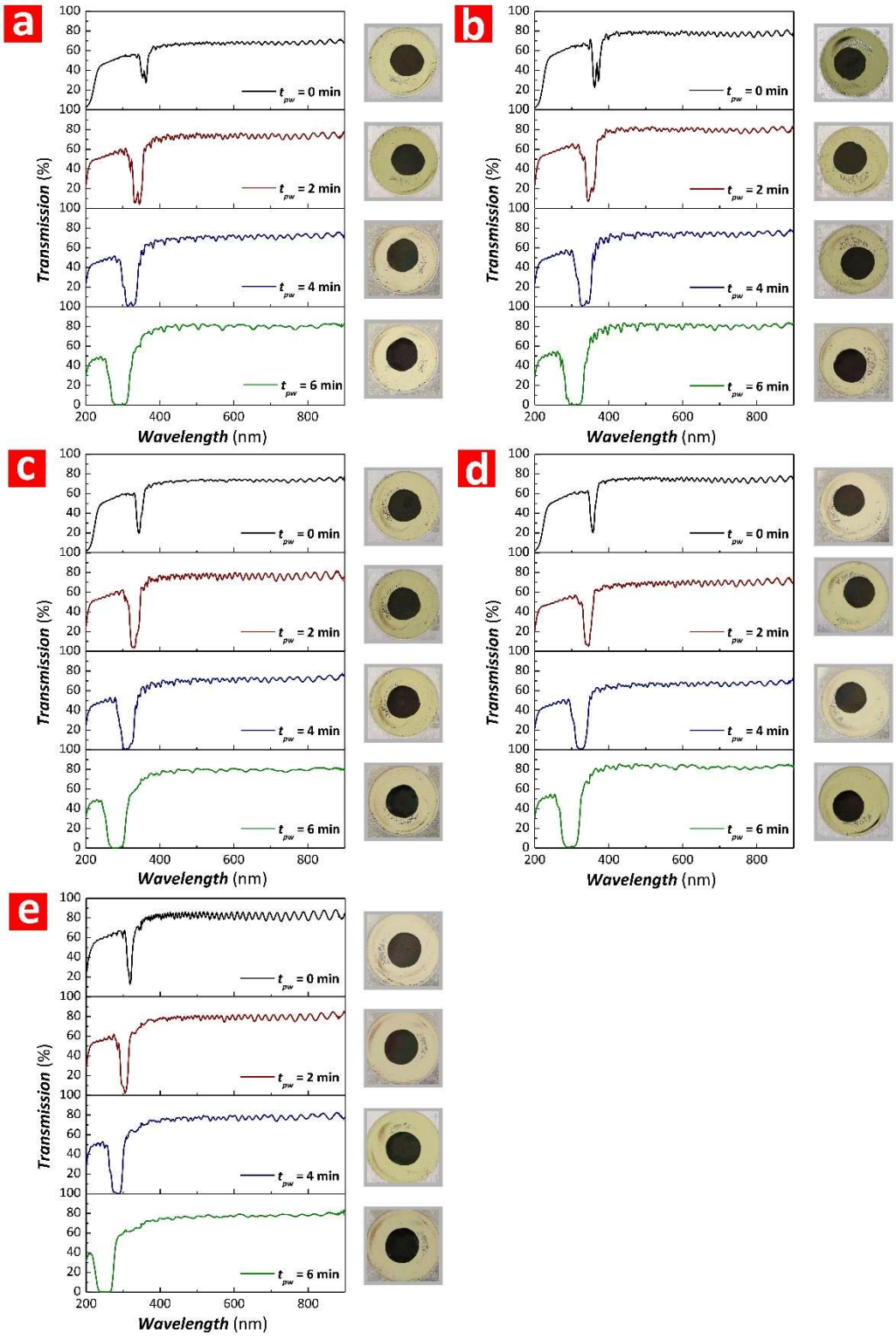


**Figure S13.** Representative transmission spectra for DBR-NAA-μCVs produced by STPA at $t_C$ = 8.5 min and variable $J_C$ and $t_{pw}$ (note: $T_P$ = 600 s, $A_J$ = 0.420 mA cm$^{-2}$, $J_{Offset}$ = 0.280 mA cm$^{-2}$, and $N_P$ = 30 pulses). a) $J_C$ = 0.210 mA cm$^{-2}$. b) $J_C$ = 0.420 mA cm$^{-2}$. c) $J_C$ = 0.315 mA cm$^{-2}$. d) $J_C$ = 0.525 mA cm$^{-2}$. e) $J_C$ = 0.630 mA cm$^{-2}$.

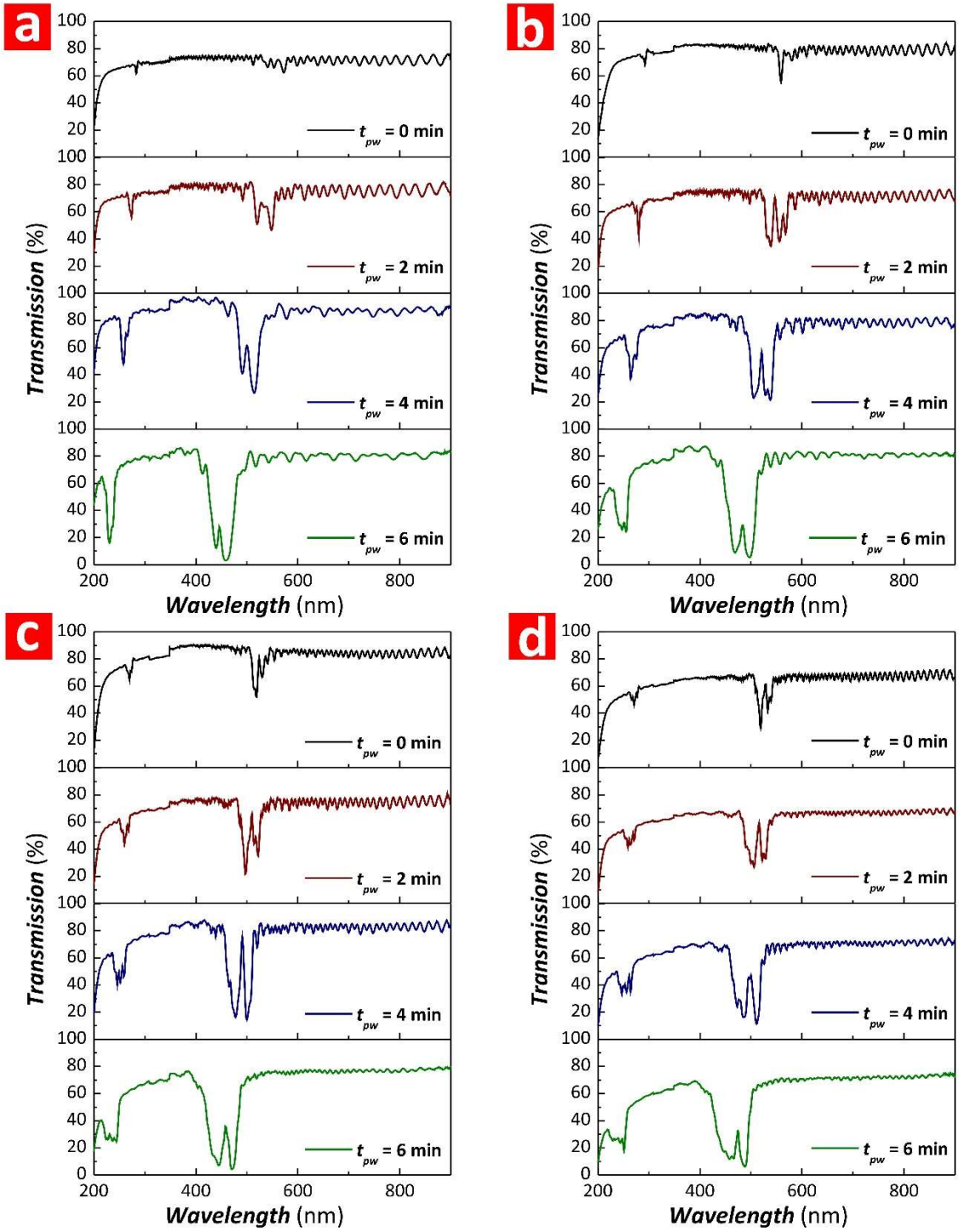


**Figure S14.** Representative transmission spectra for GIF-NAA-μCVs produced by SPA with variable $N_P$ (note: $T_P$ = 600 s, $A_J$ = 0.420 mA cm$^{-2}$, $J_{Offset}$ = 0.280 mA cm$^{-2}$, $t_C$ = 6.5 min, and $J_C$ = 0.420 mA cm$^{-2}$). a) $N_P$ = 20 pulses. b) $N_P$ = 30 pulses. c) $N_P$ = 40 pulses. d) $N_P$ = 50 pulses.

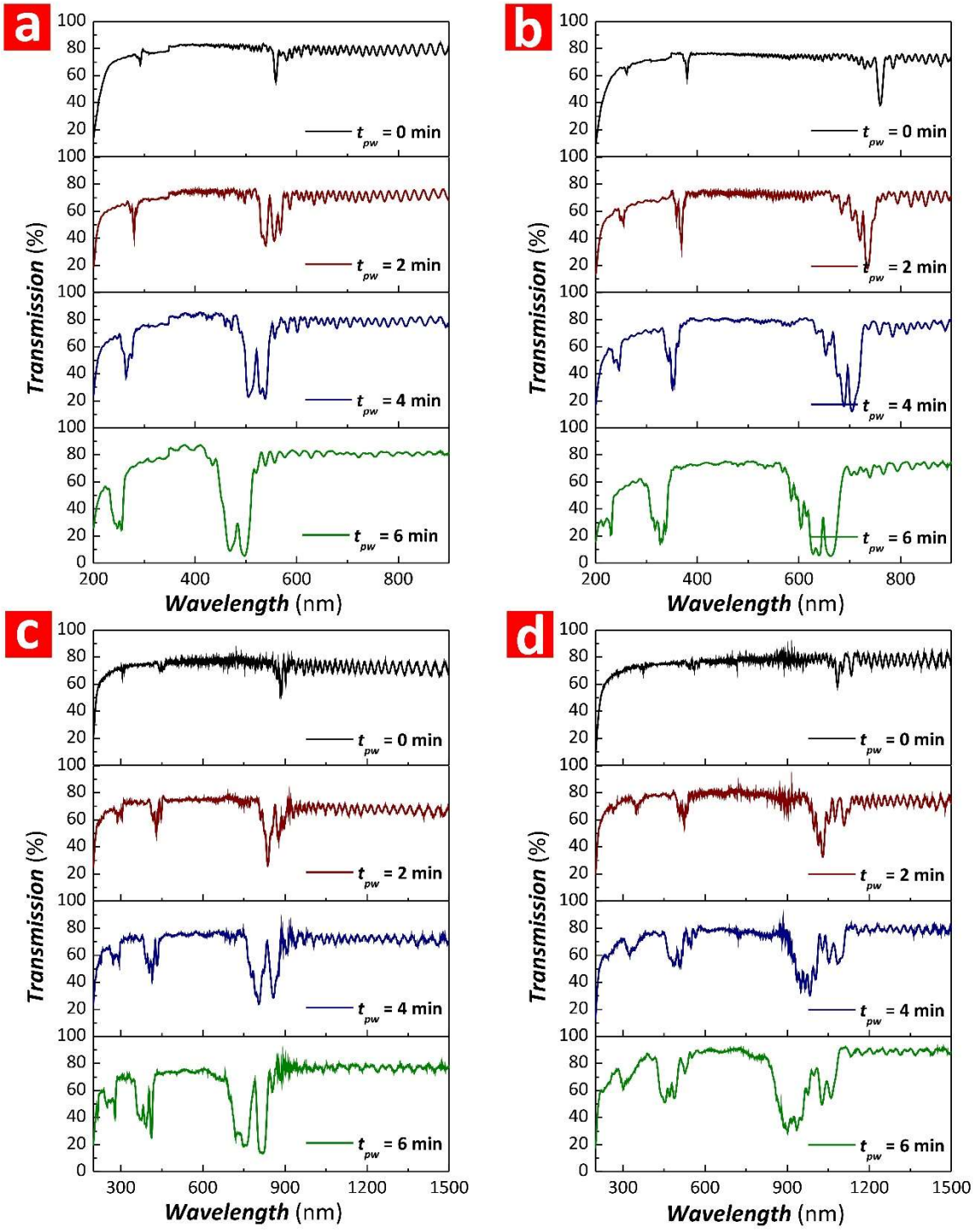


**Figure S15.** Representative transmission spectra for GIF-NAA-μCVs produced by SPA with variable $T_P$ (note: $A_J$ = 0.420 mA cm$^{-2}$, $J_{Offset}$ = 0.280 mA cm$^{-2}$, $N_P$ = 30 pulses, $t_C$ = 6.5 min, and $J_C$ = 0.420 mA cm$^{-2}$). a) $T_P$ = 600 s. b) $T_P$ = 800 s. c) $T_P$ = 1000 s. d) $T_P$ = 1200 s.